JOURNAL OF GEOPHYSICAL RESEARCH, VOL. 114, A12206, doi:10.1029/2009JA014243, 2009

Electric and magnetic field observations of Pc4 and Pc5 pulsations in the inner magnetosphere: A statistical study

W. Liu,[1,2] T. E. Sarris,[1,3] X. Li,[1,2,4] S. R. Elkington,[1] R. Ergun,[1] V. Angelopoulos,[5] J. Bonnell,[6] and K. H. Glassmeier[7,8]

Received 14 March 2009; revised 1 July 2009; accepted 21 August 2009; published 4 December 2009.

[1] Ultralow frequency (ULF) waves in the Pc4 and Pc5 bands are ubiquitous in the inner magnetosphere and have significant influence on energetic particle transport. Investigating the source and characteristics of ULF waves also helps us better understand the interaction processes between the solar wind and the magnetosphere. However, owing to the limitation in instrumentation and spatial coverage, the distribution of ULF waves in local time and L shell in the inner magnetosphere has not been completely studied. The recent Time History of Events and Macroscale Interactions During Substorms (THEMIS) mission provides unique opportunities to investigate the spatial distribution of ULF pulsations across different L shells with full local time coverage in the inner magnetosphere during solar minimum, with both electric and magnetic field measurements. Pc4 and Pc5 pulsations in the electric field observations are identified throughout 13 months of measurements, covering 24 h in local time. The pulsations are characterized as either toroidal or poloidal (including compressional) mode, depending on the polarization of the electric field. Subsequently, the pulsations' occurrence rate and wave power distributions in radial distance and local time are recorded. While the distributions of both Pc4 and Pc5 events vary greatly with radial distance and local time, Pc4 events are more frequently observed in the inner region around 5–6 R_E and Pc5 events are more frequently observed in the outer region around 7–9 R_E, which suggests that the field line resonance is an important source of the ULF waves. In the flank regions, the wave power is dominated by the toroidal mode, likely associated with the Kelvin-Helmholtz (KH) instability. In the noon sector, the Pc5 ULF wave power is dominated by the poloidal mode, likely associated with the solar wind dynamic pressure disturbance. The KH instability plays an important role, suggested by our observations, during the solar minimum when the solar wind dynamic pressure is relatively weak. We also find that the contributions to the Pc5 ULF wave power from the external sources are larger than the contributions from the internal sources. These statistical results are important in characterizing Pc4 and Pc5 waves and also important for any efforts to model the transport of energetic particles in the magnetosphere.

Citation: Liu, W., T. E. Sarris, X. Li, S. R. Elkington, R. Ergun, V. Angelopoulos, J. Bonnell, and K. H. Glassmeier (2009), Electric and magnetic field observations of Pc4 and Pc5 pulsations in the inner magnetosphere: A statistical study, *J. Geophys. Res.*, *114*, A12206, doi:10.1029/2009JA014243.

1. Introduction

[2] The frequency spectrum of ULF waves in the terrestrial magnetosphere has been studied extensively in the past using both ground-based and satellite measurements [e.g., *Jacobs et al.*, 1964; *Anderson et al.*, 1990; *Mathie et al.*, 1999; *Mann et al.*, 2002] as well as models [e.g., *Orr and Matthew*, 1971; *Singer et al.*, 1981; *Glassmeier et al.*, 1999]. Part of the great interest in these waves is that electric and magnetic perturbations in the Pc4 and Pc5 range of ULF frequencies, at 6.7–22 mHz and 1.7–6.7 mHz, respectively, can have significant influence on energetic particles (100s of keV to multiple MeV) in the magnetosphere, which have drift frequencies comparable to this range [e.g., *Fälthammar*, 1968]. The effectiveness of the interaction between ener-

[1]Laboratory for Atmospheric and Space Physics, University of Colorado at Boulder, Boulder, Colorado, USA.
[2]Laboratory for Space Weather, Chinese Academy of Sciences, Beijing, China.
[3]Space Research Laboratory, Democritus University of Thrace, Xanthi, Greece.
[4]Department of Aerospace Engineering Sciences, University of Colorado at Boulder, Boulder, Colorado, USA.
[5]IGPP, University of California, Los Angeles, California, USA.
[6]Space Sciences Laboratory, University of California, Berkeley, California, USA.
[7]IGEP, Technical University of Braunschweig, Braunschweig, Germany.
[8]Max Planck Institute for Solar System Research, Katlenburg-Lindau, Germany.

0148-0227/09/2009JA014243$09.00

getic particles and the ULF waves also depends on the polarization of the waves. For example, poloidal and compressional modes are much more effective in transporting energetic particles in radial direction than toroidal mode [e.g., *Elkington et al.*, 2003]. However, studying the polarization of ULF waves, that is, the identification and separation of poloidal, toroidal, and compressional modes of the pulsations, in contrast to their frequencies, is much more difficult. This is because of the following (often conflicting) reasons: (1) Measurements across different L shells are required, as the characteristics of ULF waves vary greatly with L shell (with field line length) [e.g., *Zhu and Kivelson*, 1991]. (2) Spacecraft measurements are required, as opposed to ground-based measurements, as some pulsations, particularly of high mode number [*Hughes and Southwood*, 1976], are screened and/or their polarization are altered by the ionosphere [e.g., *Yumoto et al.*, 1983; *Glassmeier and Stellmacher*, 2000]. (3) Measurements near the equatorial plane, as opposed to measurements along a polar orbit, are ideal in order to measure the waves at similar latitudes, as polar orbits are entwined with the difficulty of differentiating temporal effects from L shell effects. (4) Measurements with both an electric field and magnetic field are required, as the toroidal wave magnetic field has a node at the magnetic equator [e.g., *Hughes*, 1994; *Denton et al.*, 2001]. Thus, ideally a spacecraft in a highly elliptical orbit, on the equatorial plane, with both an electric and magnetic field instrument is needed to better resolve features of ULF pulsations in the magnetosphere. Furthermore, since magnetometers measure the magnetic field at a single point, the definition of wave propagation direction and wavelength is ambiguous unless multipoint measurements are made [*Takahashi et al.*, 1985; *Glassmeier et al.*, 2001] or electric field measurements are incorporated [*Clemmons et al.*, 2000]. We show in this paper that Time History of Events and Macroscale Interactions During Substorms (THEMIS) is ideal for ULF polarization studies, as it meets all the above criteria.

[3] Several statistical studies of the distribution of ULF waves in the inner magnetosphere have been performed using measurements from spacecraft that satisfied some of the above conditions. *Zhu and Kivelson* [1991] studied the properties of the ULF waves of period 2–20 min by investigating the amplitudes and polarizations based on the magnetic field and plasma data observed by ISEE 1 and 2. They concluded that intense compressional waves were a persistent feature near the two flanks of the magnetosphere and transverse waves polarized in the azimuthal direction were found to be mainly a nightside phenomenon. *Anderson et al.* [1990] used AMPTE CCE magnetic field data from L = 5 to 9 near the equatorial plane to investigate the spatial occurrence distributions of Pc3–Pc5 ULF pulsations in different categories classified by polarization and spectral density. They concluded that harmonic toroidal resonance was found to be the dominant coherent activity on the dayside and fundamental toroidal resonance was more observed in the dawn sector. *Lessard et al.* [1999] used the AMPTE IRM magnetic field data from L = 6 to 20 to investigate the occurrence rate of several types of Pc3–Pc4 pulsations. They found that fundamental resonances were observed to occur over a limited range of L shells and were not well correlated with harmonic resonances. *Hudson et al.* [2004] used CRRES magnetic field data to study the occurrence rate of Pc5 ULF oscillations in toroidal and poloidal modes. They found that there was a comparable probability of occurrence of toroidal mode oscillations on the dawn and dusk sides inside geosynchronous orbit, while poloidal mode oscillations occurred predominantly along the dusk side. *Takahashi and Ukhorskiy* [2007] statistically studied the solar wind control of the power of Pc5 magnetic pulsations at geosynchronous orbit on the basis of ACE solar wind parameters and GOES 8 magnetic field measurements. They found that solar wind dynamic pressure had the highest correlation with the magnetic pulsations at geosynchronous orbit among the solar wind parameters. Several ground-based observations were also used to investigate the statistical behavior of certain ULF pulsations (with small mode number) in the magnetosphere, such as the studies by *Glassmeier and Stellmacher* [2000] and *Mann et al.* [2002]. None of these works involved electric field observations, perhaps owing to the difficulties in the measurement of electric field. However, as discussed later in section 2, magnetic field observations alone cannot fully characterize all features of the ULF pulsations and electric field measurements are required to provide an unambiguous picture of ULF activity in the inner magnetosphere.

[4] In a paper by *Sarris et al.* [2009], it was shown that the THEMIS mission [*Angelopoulos*, 2008] provides an ideal tool for characterizing ULF pulsations, and in particular for investigating their polarization characteristics in the inner magnetosphere. The THEMIS constellation, consisting of five microsatellites hereafter termed "probes" A through E, was launched on 17 February 2007 in a low-inclination and highly elliptical orbit. The THEMIS probes were equipped with instruments that measure the electric and magnetic fields, as well as thermal and superthermal ions and electrons. For this study THEMIS measurements are used to characterize the statistical distribution and polarizations of Pc4 and Pc5 ULF waves across different L shells in the inner magnetosphere. In particular, the THEMIS electric field instruments perform measurements in the XY plane (GSE coordinates), as opposed to previous CRRES measurements which provided only one component of the electric field in the equatorial plane. Thus, using THEMIS measurements, we can calculate the radial and azimuthal electric field components, based on which we can further identify the mode of the ULF waves. *Hudson et al.* [2004] confirmed that the poloidal and compressional modes are usually mixed together. In our study, as has been done in many studies before, we do not distinguish the poloidal and compressional modes and use "poloidal mode" to represent both of them.

[5] Since the launch, the THEMIS probes traversed the inner magnetosphere in a pedaling orbit of successively larger local time of perigee. After the orbit replacement in October 2007, THEMIS D maintained an average orbital period of one day, an apogee of 12 R_E and a precession time that remained relatively constant. In this study we use THEMIS D measurements to identify and statistically analyze Pc4 and Pc5 ULF pulsations. Individual Pc4 and Pc5 pulsation events during this period were selected by an automated routine that identifies peaks in the power spectrum, using a method similar to the one used by *Takahashi*

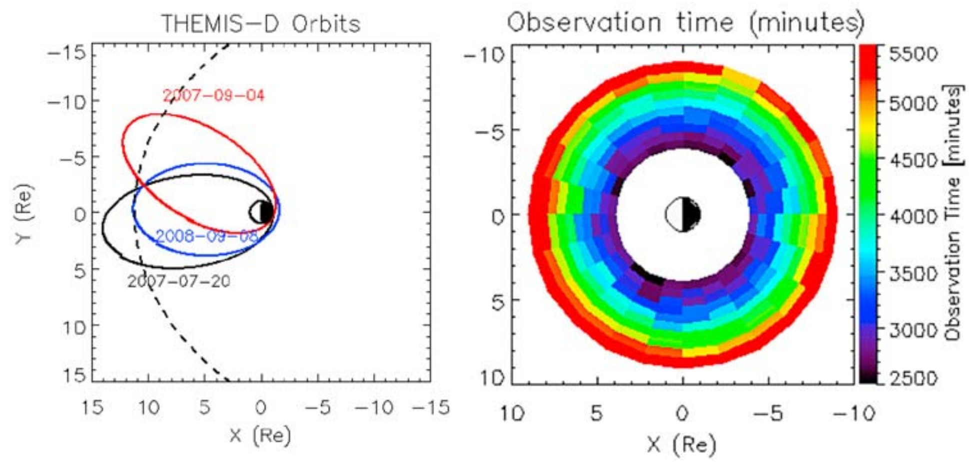

Figure 1. (left) The orbits of THEMIS-D are shown for 20 July 2007 (black), 4 September 2007 (red), and 8 September 2008 (blue). The magnetopause location (dashed line) is calculated on the basis of *Shue et al.*'s [1997] model with Bz = 1 nT and Dp = 3 nPa, as a reference. (right) The observation time in the equatorial plane is color-coded as a function of radial distance and local time.

and Ukhorskiy [2008]. In their statistical study, *Takahashi and Ukhorskiy* [2008] investigated the solar wind control of Pc5 waves at geosynchronous orbit using GOES 8 magnetic field measurements with a 1 min resolution. In this study we investigate Pc4 and Pc5 waves across a wide range of L, from the plasmapause to the magnetopause, for all local times. We show that the combined use of electric and magnetic field instruments, as provided by the THEMIS probes, is ideal for the mode identification of ULF waves, as compared to past magnetometer-only studies.

[6] In section 2 the data set used in this study is presented, including electric and magnetic field measurements from THEMIS and two examples from outbound passes of THEMIS D. In section 3 the method of extracting Pc4 and Pc5 events is described, together with the method used to produce the statistical results. In section 4 the statistical distributions of the Pc4 and Pc5 waves in the inner magnetosphere are presented. The conclusions are given in section 5.

2. Data

2.1. Orbit

[7] We use electric and magnetic field measurements from THEMIS, from November 2007 to December 2008. At each orbit, the probes were traversing the inner magnetosphere, crossing the plasmasphere, magnetosphere and magnetosheath. The local time of perigee was successively decreasing, providing within this 13 month period a complete coverage of the inner magnetosphere. We statistically characterize various features of Pc4 and Pc5 pulsations in the magnetosphere. Three examples of the trajectory of THEMIS D are shown in Figure 1 (left) for 20 July 2007 (black), 4 September 4 2007 (red), and 8 September 2008 (blue). Measurements of the electric and magnetic fields on 20 July 2007 and 8 September 2008 are discussed in section 2.2. Measurements on 4 September 2007 were presented by *Sarris et al.* [2009]. The coverage of the equatorial plane by THEMIS from November 2007 to December 2008 is shown in Figure 1 (right), where the observation time is color-coded as a function of radial distance and local time.

2.2. Electric and Magnetic Field Measurements

[8] The electric and magnetic field measurements are provided by the Electric Field Instrument (EFI) [*Bonnell et al.*, 2008] and the Fluxgate Magnetometer (FGM) [*Auster et al.*, 2008], respectively. All THEMIS satellites are equipped with identical instruments. EFIs contain two pairs of long wire booms (~40 and 50 m, respectively) extended in the spacecraft spin plane, which is approximately the $x - y$ plane in GSE, and one pair of short (~7 m) along-axis booms. The short pair of booms is not used in this analysis.

[9] Components of the electric and magnetic field vector were projected in a Mean-Field-Aligned (MFA) coordinate system from the GSE coordinate system, in order to separate the ULF field variations perpendicular to as well as along the magnetic field direction. In this system, $B_{//}$ is obtained from a 30 min running average of the magnetic field, centered at the data point being processed. The azimuthal direction, $\widehat{\mathbf{e}}_\phi$, is determined by $\widehat{\mathbf{e}}_{//} \times \vec{\mathbf{r}}_e$, where $\widehat{\mathbf{e}}_{//}$ points along the average background magnetic field direction and $\vec{\mathbf{r}}_e$ is the radial position vector, positive outward. The radial direction, with its unit director defined as $\widehat{\mathbf{e}}_r$. The vectors ($\widehat{\mathbf{e}}_r$, $\widehat{\mathbf{e}}_\phi$, $\widehat{\mathbf{e}}_{//}$) complete the orthogonal system. The oscillations in the magnetic (electric) field components projected to the $\widehat{\mathbf{e}}_r$ ($\widehat{\mathbf{e}}_\phi$) and $\widehat{\mathbf{e}}_\phi$($\widehat{\mathbf{e}}_r$) directions are referred to as poloidal mode (including compressional mode, as the B_z component is usually associated with the poloidal mode) and toroidal mode, respectively. As discussed in section 1, we do not distinguish poloidal and compressional modes. It is also necessary to clarify that the terms ''poloidal'' and ''toroidal'' are usually used to classify magnetic field oscillations [*Dungey*, 1954]. The oscillations in electric field are associated with the oscillations in magnetic field. In this paper, we use the electric field signatures to distinguish these two modes. In rotating the field components into MFA coordinates, the 30 min average acts as a high pass filter removing frequencies below 0.55 mHz, so frequencies in the Pc4 and Pc5 range are not affected.

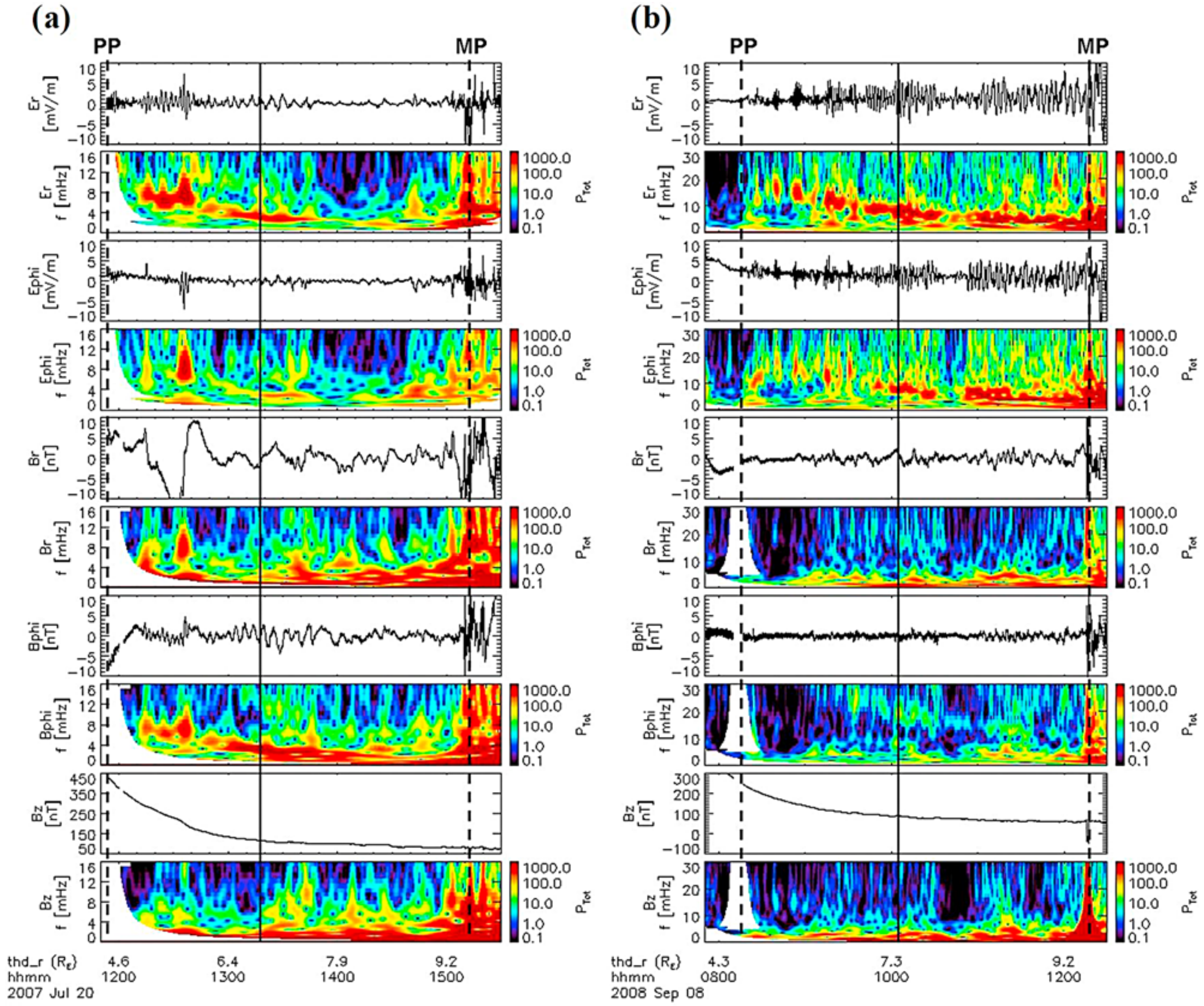

Figure 2. Two examples of electric and magnetic field measurements from THEMIS-D (a) from 1150 to 1530 UT on 20 July 2007 and (b) from 0750 to 1230 UT on 8 September 2008.

[10] The presence of significant densities of cold (<tens of eV) plasma in the magnetosphere can have impact on double-probe electric field measurements through electrostatic wake formation [*Bonnell et al.*, 2008]. The contamination in DC electric field measurements by local electrostatic fields arising from cold plasma wakes can be detected by comparing the electric field estimates from the long (E12) and short (E34) spin plane booms. The signals on the short boom antenna are larger in amplitude than that on the long booms when the wake effects are significant. The diagnostic analysis of the effects of cold plasma wakes on the power spectra in the ULF wave range has been performed in this study for several cases throughout the inner magnetosphere. It is found that the wave power spectra of the electric field estimates from the short and long booms are very similar in the frequency ranges from 2 to 30 mHz, even during the time with significant increases in the |E34|/|E12| ratio. It is thus suggested that the cold plasma wakes do not seem to have a significant effect upon the electric field power spectra in the Pc4 and Pc5 ranges (J. W. Bonnell, private communication, 2009).

2.3. Case Study A: ULF Wave Event on 20 July 2007

[11] An example of electric and magnetic field measurements from THEMIS D from 1130 to 1600 UT on 20 July 2007 is presented in Figure 2a. In Figure 2a, the radial and azimuthal electric field components, E_r and E_φ, and the radial, azimuthal, and parallel magnetic field components, B_r, B_φ, and $B_{//}$ are plotted, as marked. Data points are plotted with a $\sim$3 s resolution, corresponding to the spin period of THEMIS D. The color plots below each of the components give the corresponding dynamic power spectra (DPS) for frequencies up to 16 mHz. The DPS calculations were performed using a wavelet analysis with a Morlet wavelet [*Morlet et al.*, 1982].

[12] In this case, fluctuations at discrete frequencies in the electric and magnetic field are seen mostly in the radial component of the E field, E_r, and the azimuthal component of the magnetic field, B_φ, which suggests that ULF waves during this time are in toroidal mode. Interestingly, signatures of harmonics of these frequencies are also observed in the power spectra, as discussed by *Sarris et al.* [2009] for pulsations on 4 September 2007. For

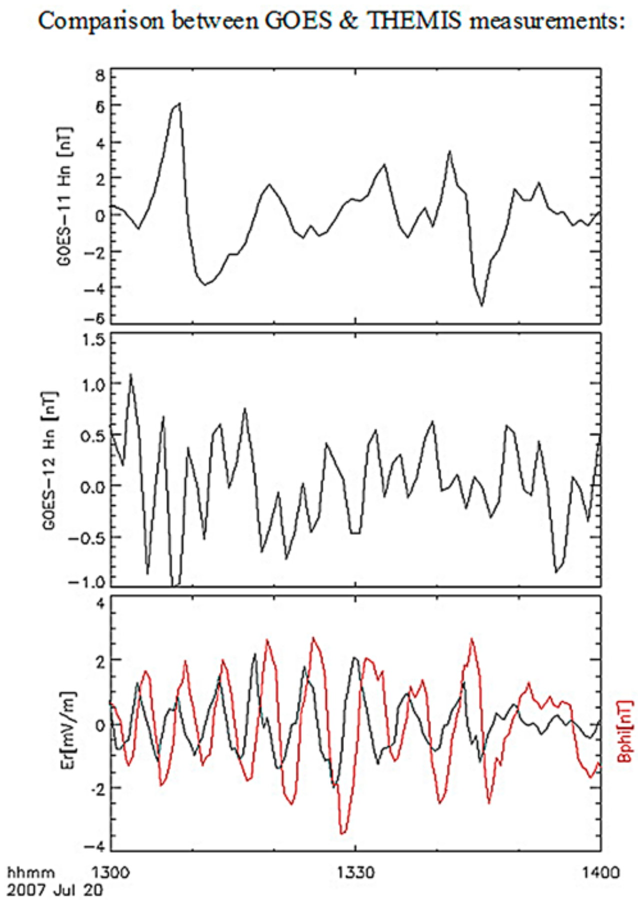

Figure 3. The fluctuations in the H_n components of (top) GOES 11 and (middle) 12 and (bottom) the azimuthal magnetic field and radial electric field of THEMIS D from 1300 to 1400 UT on 20 July 2007.

example, at 1318 UT, as marked by the solid line in Figure 2a, a clear harmonic can be distinguished in the E_r component (second panel) at a frequency of ~8 mHz, which is considered as the second harmonic of the fundamental mode at ~4 mHz. In the B_φ component (tenth panel), the harmonic is at a frequency of ~12 mHz, which is approximately 3 times the frequency of the fundamental mode and is considered as the third harmonic. In this case, the second harmonic is not clearly observed in the B_φ component.

[13] In Figure 3 (top and middle), the fluctuations of the H_n (eastward) components of GOES 11 and GOES 12 during 1300–1400 UT are plotted. These satellites observed fluctuations of different frequencies in different locations across a broad range of radial distance (4–8 R_E) and local time (0400–1100). GOES 11 was traveling at 0400–0500 LT and GOES 12 was traveling at 0800–0900 LT. GOES 11 observed low-frequency oscillations below the Pc5 range. GOES 12 observed oscillations at frequency of ~5 mHz. The radial electric field and azimuthal magnetic field measured by THEMIS D are plotted in Figure 3 (bottom) as red and black lines, respectively. The oscillations can be seen in both components at a frequency of ~3 mHz. Furthermore, from THEMIS observation, a ~90 degree phase difference can be identified between E_r and B_φ fluctuations, which suggests that this ULF wave is a standing Alfvén wave. However, such a conclusion cannot be drawn from GOES data only, without electric field measurement. This event demonstrates the advantage of THEMIS observations for ULF wave studies.

2.4. Case Study B: ULF Wave Event on 8 September 2008

[14] Another example of electric and magnetic field measurements from THEMIS D from 0800 to 1230 UT on 8 September 2008 is presented in Figure 2b, in the same format as that of Figure 2a.

[15] In this event, the discrete ULF wave activities are observed throughout the outbound orbit of THEMIS D, from the plasmapause (PP) to the magnetopause (MP), as indicated by the two dashed lines. The signature of the fundamental mode can be distinguished continuously in the electric field observations throughout this time and is clearer mostly in the E_r component, suggesting the presence of a toroidal mode of oscillation. At some time period, the oscillation in the E_φ component is comparable to, or even stronger than that in the E_r component, which perhaps suggests the mixture of toroidal and poloidal modes, as discussed by *Sarris et al.* [2009] about an event observed on 4 September 2007. In the magnetic field measurements, the fundamental mode is not observed continuously and is not as clear as it is in electric field measurements. However, strong harmonic oscillations are observed in the B_φ component at a frequency that is roughly twice the frequency of the fundamental mode observed from the E_r component. For example, at 1005 UT as marked by a solid line, the frequency of the fundamental mode is ~8.5 mHz observed from the E_r component, and the frequency of the second harmonic mode ~19 mHz observed from the B_φ component. Again, in this case, it is shown that magnetic field observations alone cannot fully characterize all features of the ULF pulsations and that electric field measurements are required to provide an unambiguous picture of ULF activity in the inner magnetosphere.

3. Statistical Analysis

3.1. Identification of Pc4 and Pc5 Events

[16] In the investigation performed, 13 months of electric field measurements were spectrally analyzed in order to detect spectral peaks in the Pc4 and Pc5 range, which would signify the appearance of narrowband toroidal or poloidal waves.

[17] In past spectral analyses of long-term data, similar methods were adopted. For example, *Glassmeier and Stellmacher* [2000] defined the "Pc5 index" as the ratio of the spectral power integrated over the approximate Pc5 band (2–8 mHz) to the spectral power integrated over the much wider 0.2–100 mHz band in order to identify the dominance of a narrowband Pc5 pulsation in a given time interval. In a different approach, *Takahashi and Ukhorskiy* [2007] defined the "toroidal wave index" as the ratio of the wave power in the toroidal component of the Pc5 waves for spectral peaks that have a full width at half maximum of less than 2 mHz, over the integrated wave power in the azimuthal component over the fixed Pc5 band, from 1.7 to 6.7 mHz. The advantage of the latter approach is that the

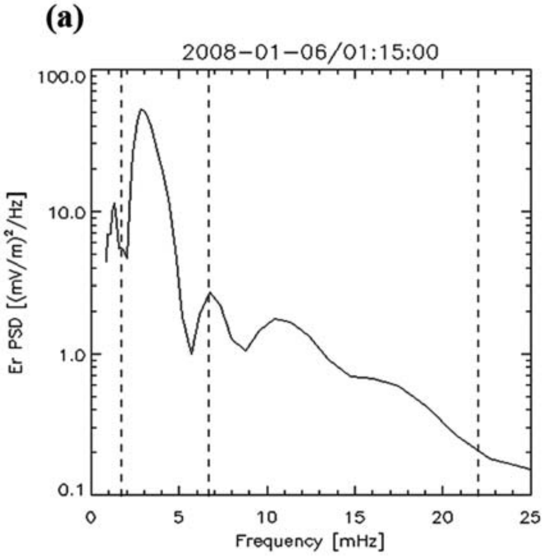

Figure 4. Two examples of a Pc5 and a Pc4 toroidal event, as selected using the criteria described in section 3.1.

frequency band changes from event to event, and that it can better identify monochromatic toroidal waves.

[18] In this work, we extend the method used by *Takahashi and Ukhorskiy* [2007], in order to identify and investigate toroidal and poloidal waves, taking advantage of the enhanced capabilities provided by the THEMIS electric field instrument. In general, identifying pulsation events appears to be much easier through the electric field instrument. One reason is that, for the case of fundamental toroidal waves, the magnetic field component of the wave has a node in the magnetic equator, making it difficult for equatorial spacecraft such as THEMIS (and also GOES geosynchronous satellites) to detect the fundamental mode of field line resonances (FLRs, the "Alfvén continuum" that has wave frequency varying continuously with respect to L) through magnetic field measurements [e.g., *Singer and Kivelson*, 1979]. On the other hand, the electric field component of the wave has an antinode, and thus maximum wave amplitude at the magnetic equator, making it easier to detect the fundamental mode and other odd harmonics, whereas the magnetic field measurements are better for detecting even harmonics.

[19] To identify wave events, the following empirical criteria are used for the power spectral density (PSD) computed from the radial and azimuthal components of electric field, projected in the mean field aligned coordinate system. The power spectrum of the azimuthal and radial electric field components, E_r and E_φ are calculated using a wavelet analysis with a Morlet wavelet. We identify spectral peaks (f_{peak}) in the Pc4 and Pc5 bands of the E_r and E_φ components by recording the maximum in the power spectral density of electric field signal in the 6.7–22 mHz and 1.7–6.7 mHz, respectively. A spectral peak is identified as an "event" if the peak is found in the electric field and the peak's full width at half maximum (FWHM, the distance between f_{lower} and f_{upper}) of the spectral peak is narrower than a threshold, which is set to 40% of the frequency at the peak. A minimum threshold of 2 mHz is employed when the peak frequency is below 5 mHz. The peak is identified as a Pc4 (Pc5) toroidal event if the peak is found in the E_r component and the power in the E_r component integrated over the Pc4 (Pc5) range is greater than the integral power in the E_φ component. Similarly, the peak is identified as a Pc4 (Pc5) poloidal event if the peak is found in the E_φ component and the power in the E_φ component integrated over the Pc4 (Pc5) range is greater than the integral power in the E_r component. We exclude the events with extremely large integral power in the Pc4 or Pc5 range (>3×10^4 (mV/m)^2/Hz), which frequently occurs during magnetopause crossings.

[20] Two examples of a toroidal Pc4 event and a toroidal Pc5 event as selected using the above criteria are shown in Figures 4a and 4b around 0115 UT of 16 January 2008 and 1955 UT of 6 September 2007, respectively. In Figures 4a and 4b, the PSD spectra of the E_r components are plotted. The dashed lines indicate the Pc4 and Pc5 ranges. In Figure 4a, a PSD peak at ~3 mHz is identified, having a FWHM of 1.5 mHz, and in Figure 4b, a PSD peak at ~10 mHz is identified, having a FWHM of 4 mHz.

3.2. Application to Case Studies

[21] Figure 5 shows a benchmark of this method applied on the FLR event discussed by *Sarris et al.* [2009]. The first and second panels of Figure 5 are the wave power spectra of the radial and azimuthal component of the electric field. The third panel is the ULF mode identified by this method, given a value of 1 for a poloidal mode event, and 2 for toroidal mode event. The fourth panel shows the integral power of E_r and E_φ in the Pc5 band. The fifth and sixth panels show frequencies f_{peak}, f_{lower} and f_{upper} of the E_r and E_φ spectra.

[22] From Figure 5, we can see that the toroidal and poloidal mode events are well identified. Before 0745UT, most of the events are poloidal. After that, most of the events are toroidal. This is consistent with the analysis result of *Sarris et al.* [2009].

[23] Figure 6 shows another example of the identification of the mode of ULF waves on 20 July 2007 in the same

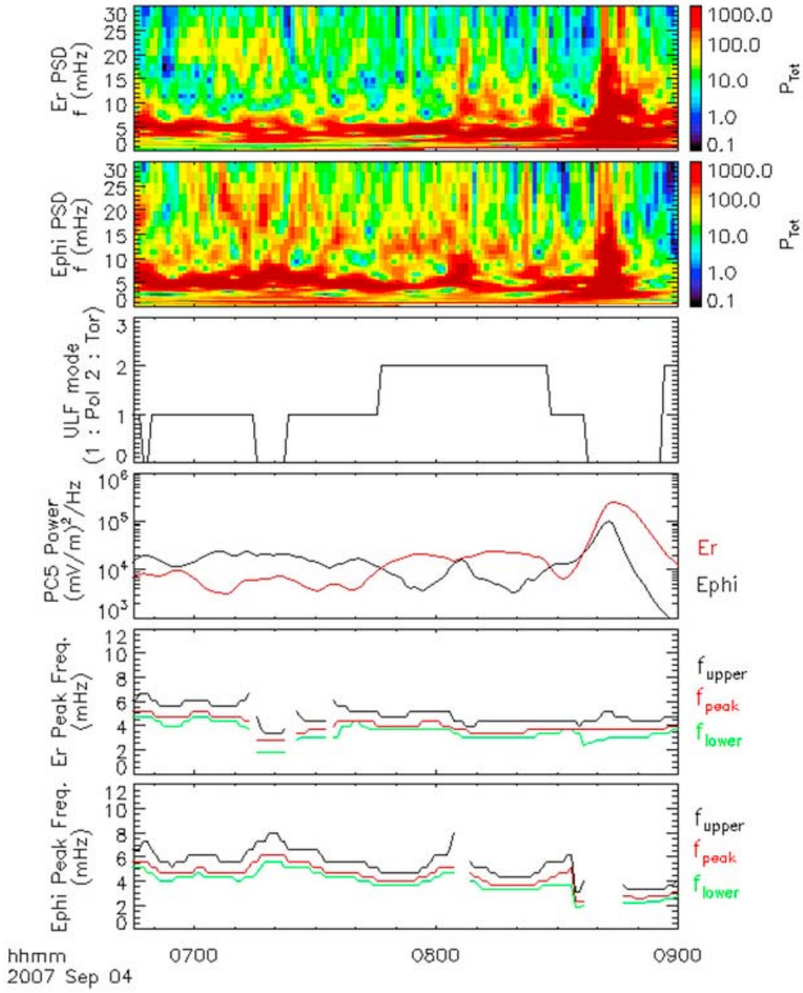

Figure 5. ULF mode identification on 4 September 2007. The first and second panels are the wave power spectra of the radial and azimuthal component of the electric field. The third panel is the ULF mode identified by this method, given a value of 1 for a poloidal mode event and 2 for toroidal mode event. The fourth panel shows the integral power of E_r and E_φ in the Pc5 band. The fifth and sixth panels show frequencies f_{peak}, f_{lower}, and f_{upper} of the E_r and E_φ spectra.

format of Figure 5, in which toroidal events are dominant. A PSD peak at 3–5 mHz frequency can be clearly identified in the spectrum of E_r component from 1240 to 1350 UT, which is classified as Pc5 toroidal mode.

3.3. Statistical Analysis of Pc4 and Pc5 Toroidal and Poloidal Events

[24] The spectral and component analysis that was performed on the three selected case studies, as was presented in section 2, shows that the characteristics of Pc4 and Pc5 toroidal and poloidal pulsations vary greatly with spacecraft location. We performed the same analysis for thirteen months of THEMIS data, from November 2007 to December 2008, in order to identify the radial distance, local time and solar wind dependence of Pc4 and Pc5 toroidal and poloidal pulsation events. The minute averaged values of power spectra density are used in the analysis and one minute averaged value is considered as one sample. During this time period, the total observation time with available data was 183,375 min. In these samples, 9805 events were identified as Pc4 ULF wave events, including 4805 events in poloidal mode, and 5005 events in toroidal mode. A total of 50,184 events were identified as Pc5 ULF wave events, including 20,715 events in poloidal mode and 29,469 events in toroidal mode. We note here that, by using different statistical samples of minute and 10 min averaged values of power spectra density as input, we reach results similar to those presented in this paper. In the statistical results, the selected variables were averaged in bins of 0.5 R_E from 4 to 9 R_E in radial distance and 15 degrees in azimuth.

3.3.1. Occurrence Rate

[25] The occurrence rate is calculated from the number of events of each bin divided by the time that the spacecraft spent in that particular bin, resulting in a quantity that counts the possibility of observing a toroidal or poloidal event. The occurrence rate is plotted in Figures 7a and 7b for Pc4 events and in Figures 7c and 7d for Pc5 events. Figures 7a and 7c correspond to the poloidal mode, and Figures 7b and 7d correspond to the toroidal mode.

3.3.2. Wave Power and Peak Frequency Distribution

[26] In order to find the distribution of Pc4 and Pc5 wave power in the inner magnetosphere, we plotted the square

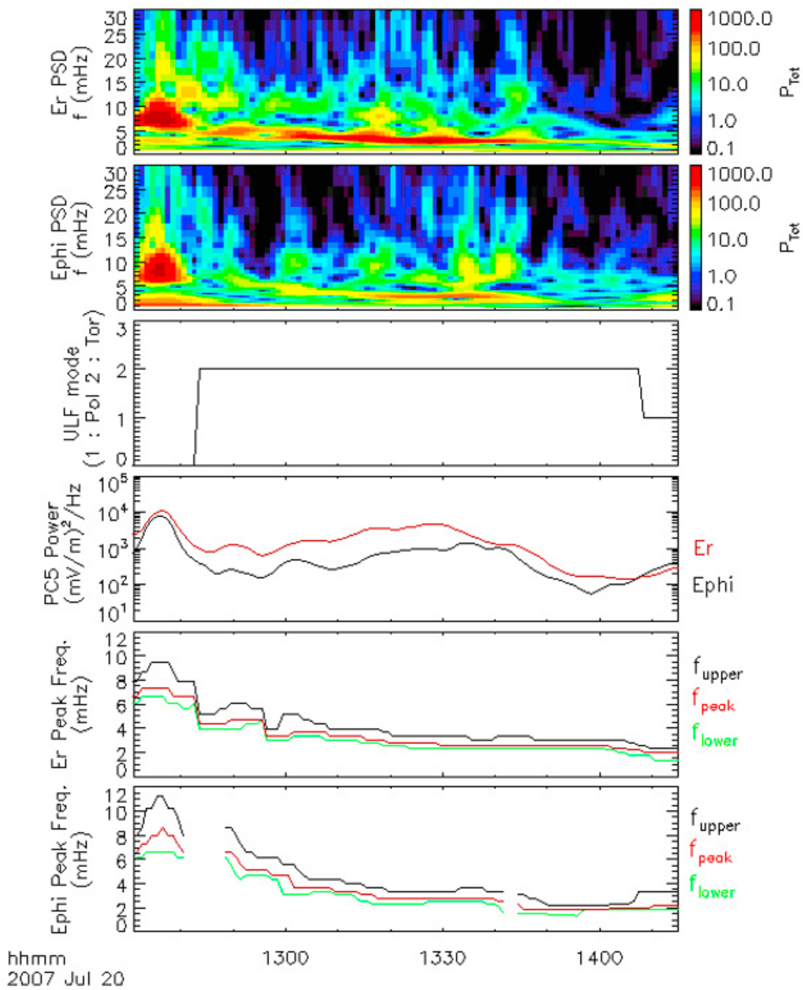

Figure 6. ULF mode identification on 20 July 2007, with the same format as that of Figure 5.

root of the integral of the power spectral density over Pc4 and Pc5 bands in Figure 8 as

$$\delta E_r = \left(\int_{f_1}^{f_2} PSD\_E_r(f)df \right)^{1/2}, \ \delta E_\varphi = \left(\int_{f_1}^{f_2} PSD\_E_\varphi(f)df \right)^{1/2}, \tag{1}$$

where δE_r and δE_φ are in units of mV/m. Figures 8a and 8b are for Pc4 events, and Figures 8c and 8d are for Pc5 events. Figures 8a and 8c are for poloidal mode, and Figures 8b and 8d are for toroidal modes.

[27] In Figure 9, we plot the distribution of the averaged value of the peak frequencies of the events observed in each sector for poloidal and toroidal modes. These statistical results will be discussed in detail in section 4, following the discussion of individual cases.

4. Discussion

4.1. On the Characterization of Pulsations

[28] In sections 2.3 and 2.4, we presented two ULF wave events which show signatures of FLRs, as confirmed also by the ~90 degree phase difference between the radial component of the electric field and the azimuthal component of the magnetic field which was shown in Figure 3. The frequencies of the fundamental and harmonic modes of the FLRs depend on the length of the field line and the Alfvén velocity along the field line [e.g., *Waters et al.*, 2000]. In the case on 20 July 2007, the FLR frequency gradually drops from 15 mHz at 4.5 R_E to 3 mHz at 9 R_E, from Pc4 range to Pc5 range. In the case on 8 September 2008, the resonance frequency decreases from 16 mHz at 4.5 R_E to 4 mHz at 9 R_E. These results, combined with the statistical analysis that is performed and presented in sections 4.2–4.5, suggest that the fundamental mode of FLR could be a significant fraction of the observed Pc4 pulsations, especially in the region outside of the plasmapause.

[29] The harmonics of FLRs are also a significant fraction of the observed Pc4 pulsations in the outer region. In the event discussed in section 2.3, at 1318 UT on 20 July 2007, as marked by the solid line in Figure 2a, the second harmonic can be distinguished in the E_r component at a frequency of ~8 mHz, and the third harmonic can be distinguished in the B_φ component at a frequency of ~12 mHz at 6.9 R_E. Both events fall into the Pc4 frequency range.

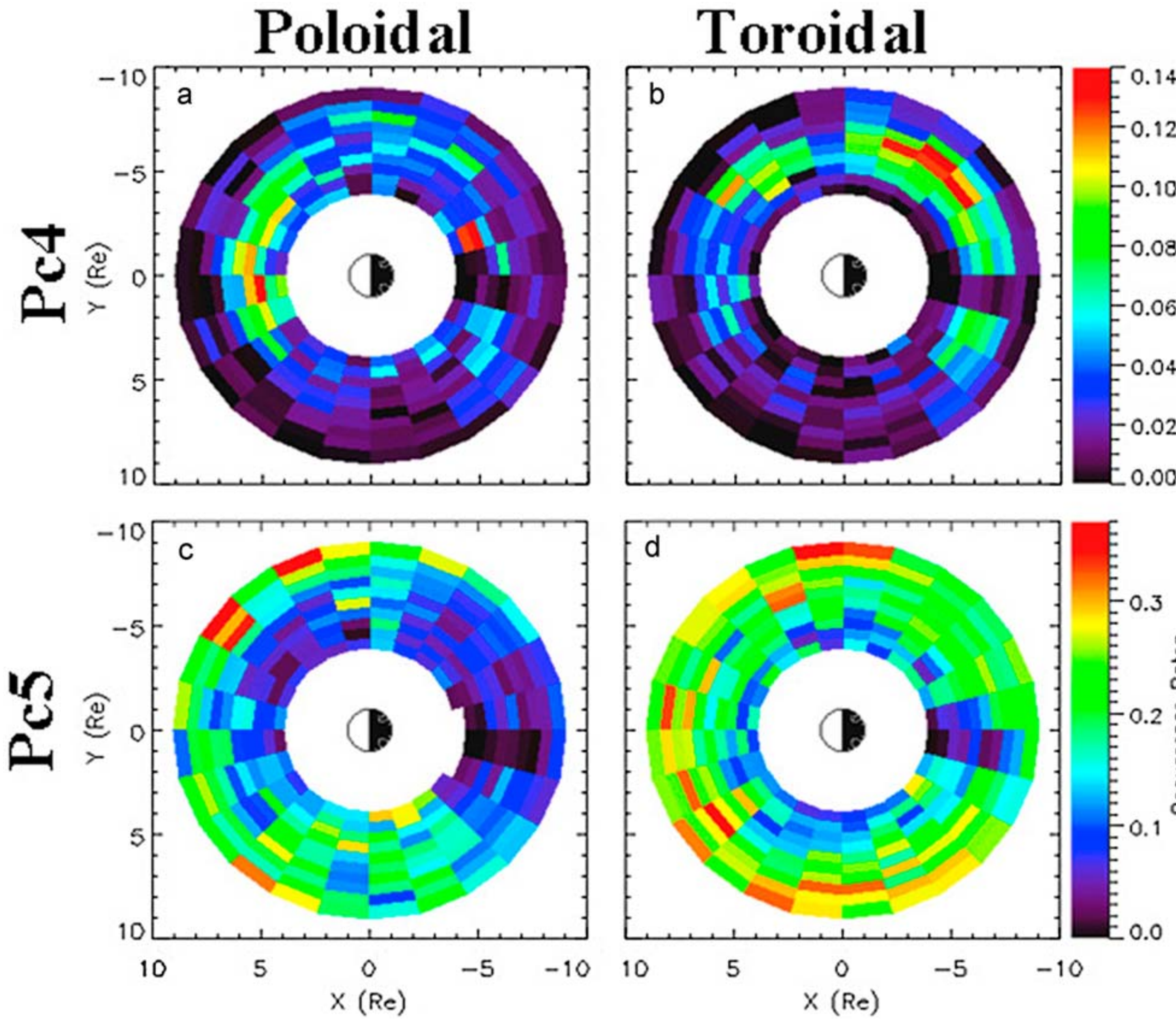

Figure 7. Statistical results of the occurrence rates of (a and b) Pc4 and (c and d) Pc5 poloidal and toroidal mode ULF waves.

[30] In the FLR event on 8 September 2008 as shown in Figure 2b, after the satellite crossed the plasmapause at around 0820 UT, strong ULF wave activity was observed in both E_r and E_φ components. The amplitudes (δE_r and δE_φ, as defined in section 3.3.2) over Pc4 and Pc5 range increase from 0.23 mV/m inside plasmapause to 1.56 mV/m outside plasmapause in the radial component and 0.19 to 1.33 mV/m in the azimuthal component. In the FLR event on 4 September 2007 as discussed by *Sarris et al.* [2009], similar results were observed. The amplitudes increase from 0.11 to 1.26 mV/m in the radial component and 0.21 to 1.03 mV/m in the azimuthal component. This amplitude behavior across the plasmapause is qualitatively consistent with the model results by *Waters et al.* [2000] and is confirmed by the statistical results in Figure 8, which shows that the wave power is relatively lower inside the plasmasphere. This behavior also suggests a new possibility to identify the plasmapause location based on the ULF wave measurements on the electric field.

4.2. On the Occurrence Rate of Pulsations

[31] From Figure 7, we can see that the occurrence rate is quite different across different L shells and local times. Overall, Pc5 events have a higher occurrence rate than Pc4 events by a factor about 2. Pc4 events are more frequently observed in the inner region around 5–6 R_E and Pc5 events are more frequently observed in the outer region around 7–9 R_E, which is likely associated with the local FLR frequency in different regions, as discussed in section 4.1. It also suggests that FLRs are an important fraction of the observed Pc4 pulsations in the inner magnetosphere and of Pc5 pulsations in the outer magnetosphere.

[32] As discussed above, the Pc4 wave activities were observed as soon as the satellite moved away from plasmasphere, suggesting that the plasmapause location can play a role in the occurrence rate of the Pc4 ULF waves. In the statistical results of both Pc4 poloidal and toroidal modes, the occurrence rate is very low in the dusk sector. This may be owing to the plasmapause location, which is generally asymmetric and often extends farther in the dusk side.

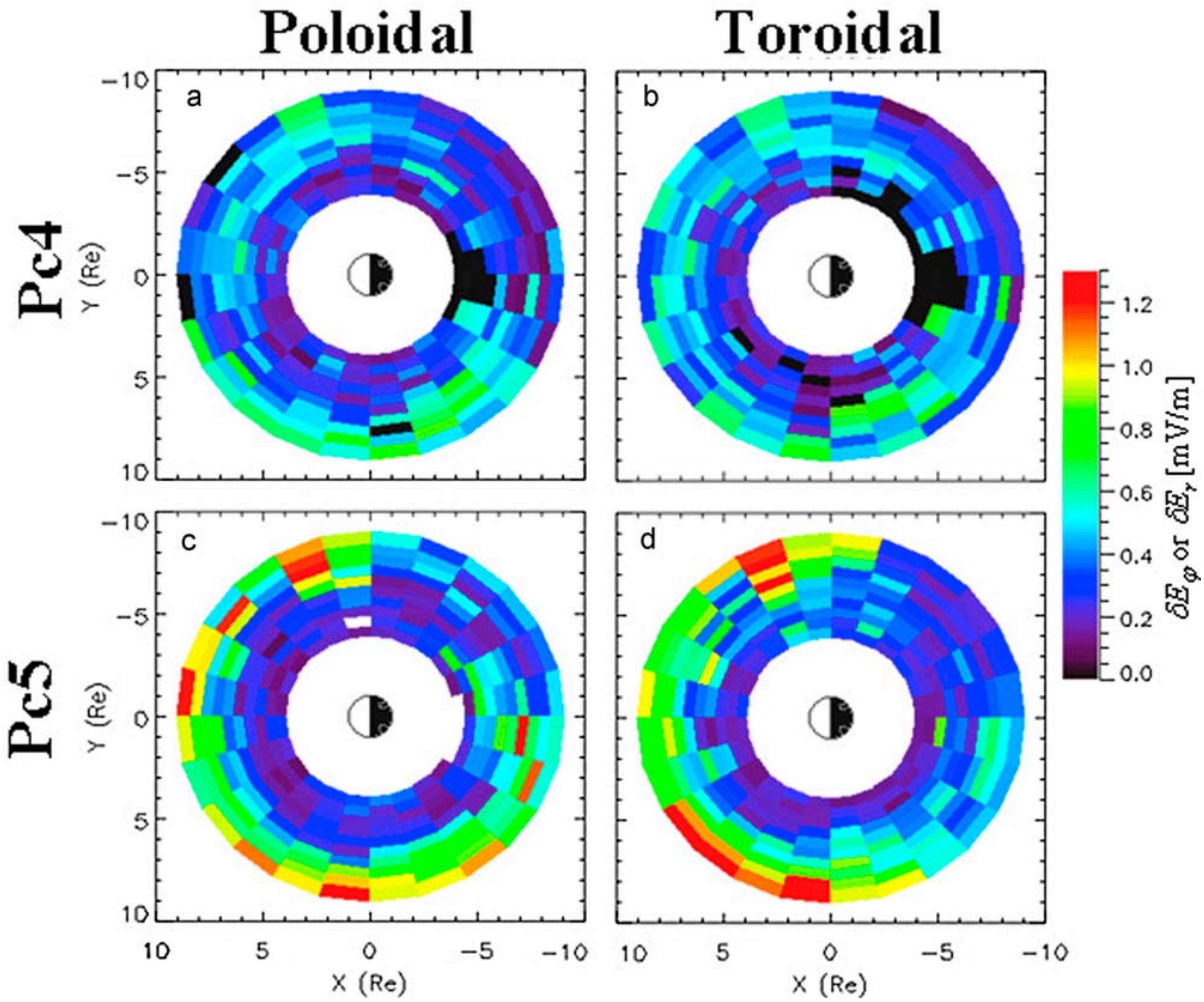

Figure 8. Statistical results of the averaged wave power. The wave power is plotted as the square root of the integral of the power spectral density over (a and b) Pc4 and (c and d) Pc5 bands.

[33] In the occurrence rate distribution of poloidal Pc5 waves (Figure 7c), the occurrence rate is clearly higher in the dusk sector than that in the dawn sector inside 8 R_E. For the toroidal mode (Figure 7d), there is no clear enhancement in the dusk sector. This supports the previous understanding that the drift resonance involving westward drifting ions from the magnetotail can excite poloidal mode Pc5 waves in the dusk sector.

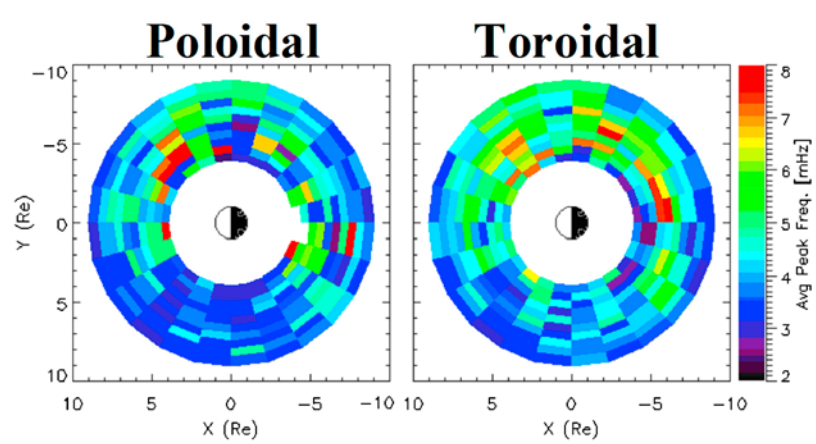

Figure 9. The distribution of the average value of the peak frequencies of the Pc4 and Pc5 events observed in each sector.

[34] Pc4 poloidal events (Figure 7a) are more frequently observed in the noon sector, whereas Pc4 toroidal events (Figure 7b) are more frequently observed in the dawn sector. The poloidal mode is more likely associated with the activities in the dayside, such as solar wind dynamic pressure disturbances, and the toroidal mode is more likely associated with the activities in the flank regions, such as the Kelvin-Helmholtz (KH) instability due to velocity shear. We cannot see a clear flank-noon difference in the occurrence of Pc5 wave. However, as will be discussed in section 4.3, we find that the wave power is stronger in the flank regions for the toroidal mode.

4.3. On the Wave Power Distribution

[35] The wave power distribution for both Pc4 and Pc5 waves varies greatly with radial distance and local time. In general, we find that the wave power in the Pc5 band is stronger than power in the Pc4 band. It is also clear that the power of both toroidal and poloidal Pc5 waves decreases with decreasing radial distance, which is consistent with the results from MHD simulations conducted by *Claudepierre et al.* [2008, 2009].

[36] For the Pc5 toroidal events (Figure 8d), the wave power is stronger at the two flank regions, where the KH instability is expected to be strong, [e.g., *Pu and Kivelson*, 1983; *Fujita et al.*, 1996; *Engebretson et al.*, 1998]. For the Pc5 poloidal events (Figure 8c), the wave power is enhanced in the noon sector but comparable to the power in the flank regions, which may be owing to the relatively weak disturbance in solar wind dynamic pressure during solar minimum. Overall, the comparison between Figures 8c and 8d suggests that, in the noon sector, the Pc5 ULF wave power is dominated by the poloidal mode and in the flank regions, the wave power is dominated by the toroidal mode.

[37] In the nightside, an overall dawn-dusk asymmetry can be distinguished in Figures 8a–8d, and the wave power is stronger in the premidnight sector. This is consistent with previous understanding that earthward plasma flow (e.g., bursty bulk flow) is a source of ULF waves during substorms [e.g., *McPherron*, 2005].

4.4. On the Peak Frequency of Pulsations

[38] In Figure 9, we plotted the distribution of the averaged value of the peak frequencies of the Pc4 and Pc5 events observed in each sector for the poloidal and toroidal modes. It is clear that the observed peak frequency decreases with radial distance, which is consistent with the peak frequency profile of FLR events, as discussed earlier in sections 2.3, 2.4, and 4.1. *Kivelson et al.* [1984, 1997] reported cavity mode events with compressional oscillations of nearly constant frequency from L $\sim$ 5 to L $\sim$ 10 near local noon. However, this type of event is difficult to observe because the cavity properties are always changing in response to the changing solar wind [*McPherron*, 2005]. In the time period we studied, we could not visually distinguish any clear cavity mode event. A large fraction of the ULF waves in this statistical study are FLRs during this solar minimum year.

[39] A dawn-dusk asymmetry can also be clearly seen as the average frequency is higher in the dawn sector than in the dusk sector by a factor of 2. *Takahashi and McPherron* [1982] observed similar results in their study for Pc5 events. In the dusk side, the lower frequency of poloidal waves is related to the lower (higher) occurrence rate of Pc4 (Pc5).

4.5. On the Sources of the ULF Waves in the Inner Magnetosphere

[40] There are various possible source mechanisms for Pc4 and Pc5 pulsations. The Pc4 and Pc5 events used in our statistical study may be the results of (1) dynamic pressure effects of the solar wind on the magnetopause, (2) the KH instability in the magnetosphere flanks, (3) plasma instabilities, or (4) the drift-bounce resonance mechanism.

[41] The interaction between the solar wind and the magnetopause is an important external source of ULF waves. The dynamic pressure fluctuations can periodically move the magnetopause in and out, and globally increase and decrease the internal magnetic field, which will excite mainly poloidal waves in the noon sector, as shown in Figure 8. The KH instability can grow on the magnetopause in the flank regions and transfer energy to the magnetosphere, which will excite mainly toroidal waves in the flank regions, as shown in Figure 8. This is consistent with fluctuations of the magnetopause along the direction of the solar wind, leading to inward motion at noon, and sheared motion at the flanks.

[42] *Takahashi and Ukhorskiy* [2008] performed correlation and superposed epoch analyses of the solar wind control parameters measured by the ACE spacecraft and the amplitude of Pc5 waves and the flux of radiation belt electrons measured at the GOES 12 geosynchronous satellite with the data observed in year 2006. They concluded that the major driver of geosynchronous Pc5 waves was solar wind pressure variations rather than the KH on the magnetopause. However, in our study, the clear intensification of toroidal Pc5 wave power in the flank regions suggests that the KH instability on the magnetopause also plays an important role in the excitation of the ULF waves in the solar minimum years. We argue that the toroidal mode ULF wave has a node in magnetic field at the magnetic equatorial plane and the conclusion will be biased if only based on the low-latitude magnetic field measurements.

[43] Several internal sources can also be distinguished in the statistical results, as shown earlier. The westward drift ions from the magnetotail can excite the poloidal mode Pc5 wave in the dusk sector owing to the drift-bounce resonance. The earthward plasma flow is a source of ULF waves during substorms. However, from Figure 8, it is suggested that the contributions of these internal sources are smaller than those of the external sources. The energy of the ULF waves in the inner magnetosphere mostly comes from the solar wind, which is consistent with *Kessel* [2008]. They examined the importance of solar wind excitation as a source of magnetospheric and ground Pc5 fluctuations, and concluded that, during the declining phase of the solar cycle in March and April 2002, external forcing due to solar wind dynamic pressure fluctuations was dominant over internal forcing.

5. Summary and Conclusions

[44] This paper reports the characteristics of Pc4 and Pc5 ULF waves in the inner magnetosphere, determined

from both electric and magnetic field measurements from THEMIS, which traverses different L shells with full local time coverage in the inner magnetosphere within one year. The distributions of the occurrence rate, wave power, and peak frequency of the ULF wave events are presented over the radial distance range of 4–9 R_E and with full local time coverage. Through this analysis, we found the following.

[45] The distribution of Pc4 and Pc5 events vary greatly with radial distance and local time in the inner magnetosphere. Pc4 events are more frequently observed in the inner regions of the magnetosphere, around 5–6 R_E, while Pc5 events are more frequently observed in the outer regions around 7–9 R_E, suggesting that the FLR is an important fraction of the observed Pc4 ULF pulsations, especially in the inner region outside of the plasmapause. The harmonic modes of FLRs possibly contribute to the observed Pc4 ULF pulsations in the outer magnetosphere.

[46] In the flank regions, the wave power is dominated by the toroidal mode, likely associated with the KH instability. In the noon sector, the Pc5 ULF wave power is dominated by the poloidal mode, likely associated with the solar wind dynamic pressure disturbance. The KH instability plays an important role, suggested by our observations, during the solar minimum when the solar wind dynamic pressure is relatively weak. These statistical results are important in characterizing Pc4 and Pc5 waves and are also important for any efforts to model the transport of energetic particles in the magnetosphere.

[47] **Acknowledgments.** This work is supported by the NASA THEMIS (NAS5-02099) project. We acknowledge NOAA SEC and CDAWeb for making GOES magnetometer data available. The work by K.H.G. was financially supported by the German Zentrum für Luft- und Raumfahrt under grant 50QP0402. This work was also supported by grants from the National Natural Science Foundation of China (40621003 and 40728005).

[48] Zuyin Pu thanks Richard Denton and Colin Waters for their assistance in evaluating this paper.

References

Anderson, B. J., M. J. Engebretson, S. P. Rounds, L. J. Zanetti, and T. A. Potemra (1990), A statistical study of Pc3–5 pulsations observed by the AMPTE/CCE magnetic field experiment: 1. Occurrence distributions, *J. Geophys. Res.*, *95*, 10,495, doi:10.1029/JA095iA07p10495.

Angelopoulos, V. (2008), The THEMIS mission, *Space Sci. Rev.*, *141*, 5, doi:10.1007/s11214-008-9336-1.

Auster, H. U., et al. (2008), The THEMIS fluxgate magnetometer, *Space Sci. Rev.*, *141*, 235, doi:10.1007/s11214-008-9365-9.

Bonnell, J. W., F. S. Mozer, G. T. Delory, A. J. Hull, R. E. Ergun, C. M. Cully, V. Angelopoulos, and P. R. Harvey (2008), The Electric Field Instrument (EFI) for THEMIS, *Space Sci. Rev.*, *141*, 303, doi:10.1007/s11214-008-9469-2.

Claudepierre, S. G., S. R. Elkington, and M. Wiltberger (2008), Solar wind driving of magnetospheric ULF waves: Pulsations driven by velocity shear at the magnetopause, *J. Geophys. Res.*, *113*, A05218, doi:10.1029/2007JA012890.

Claudepierre, S. G., M. Wiltberger, S. R. Elkington, W. Lotko, and M. K. Hudson (2009), Magnetospheric cavity modes driven by solar wind dynamic pressure fluctuations, *Geophys. Res. Lett.*, *36*, L13101, doi:10.1029/2009GL039045.

Clemmons, J. H., et al. (2000), Observations of traveling Pc5 waves and their relation to the magnetic cloud event of January 1997, *J. Geophys. Res.*, *105*, 5441, doi:10.1029/1999JA900418.

Denton, R. E., M. R. Lessard, R. Anderson, E. G. Miftakhova, and J. W. Hughes (2001), Determining the mass density along magnetic field lines from toroidal eigenfrequencies: Polynomial expansion applied to CRRES data, *J. Geophys. Res.*, *106*, 29,915, doi:10.1029/2001JA000204.

Dungey, J. W. (1954), The attenuation of Alfvén waves, *J. Geophys. Res.*, *59*, 323, doi:10.1029/JZ059i003p00323.

Elkington, S. R., M. K. Hudson, and A. A. Chan (2003), Resonant acceleration and diffusion of outer zone electrons in an asymmetric geomagnetic field, *J. Geophys. Res.*, *108*(A3), 1116, doi:10.1029/2001JA009202.

Engebretson, M., K.-H. Glassmeier, M. Stellmacher, W. Hughes, and H. Lühr (1998), The dependence of high-latitude PcS wave power on solar wind velocity and on the phase of high-speed solar wind streams, *J. Geophys. Res.*, *103*, 26,271, doi:10.1029/97JA03143.

Fälthammar, C.-G. (1968), *Radial Diffusion by Violation of the Third Adiabatic Invariant, Earth's Particles and Fields; Proceedings of the NATO Advanced Study Institute Held at Freising, Germany, July 31–August 11, 1967*, edited by B. M. McCormac, 157 pp., Reinhold, New York.

Fujita, S., K.-H. Glassmeier, and K. Kamide (1996), MHD waves generated by the Kelvin-Helmholtz instability in a nonuniform magnetosphere, *J. Geophys. Res.*, *101*, 27,317, doi:10.1029/96JA02676.

Glassmeier, K.H., and M. Stellmacher (2000), Concerning the local time asymmetry of Pc5 wave power at the ground and field line resonance width, *J. Geophys. Res.*, *105*, 18,847, doi:10.1029/2000JA900037.

Glassmeier, K.-H., et al. (1999), Magnetospheric field line resonances: A comparative planetology approach, *Surv. Geophys.*, *20*, 61.

Glassmeier, K.-H., et al. (2001), Cluster as a wave telescope: First results from the fluxgate magnetometer, *Ann. Geophys.*, *19*, 1439.

Hudson, M. K., R. E. Denton, M. R. Lessard, E. G. Miftakhova, and R. R. Anderson (2004), A study of Pc-5 ULF oscillations, *Ann. Geophys.*, *22*, 289.

Hughes, W. J. (1994), Magnetospheric ULF waves: A tutorial with a historical perspective, in *Solar Wind Source of Magnetosphere Ultra-Low-Frequency Waves*, *Geophys. Monogr. Ser.*, vol. 81, edited by M. J. Engebretson et al., p. 25, AGU, Washington, D. C.

Hughes, W. J., and D. J. Southwood (1976), The screening of micropulsation signals by the atmosphere and ionosphere, *J. Geophys. Res.*, *81*, 3234, doi:10.1029/JA081i019p03234.

Jacobs, J. A., Y. Kato, S. Matsushita, and V. A. Troitskaya (1964), Classification of geomagnetic micropulsations, *J. Geophys. Res.*, *69*, 180, doi:10.1029/JZ069i001p00180.

Kessel, R. L. (2008), Solar wind excitation of Pc5 fluctuations in the magnetosphere and on the ground, *J. Geophys. Res.*, *113*, A04202, doi:10.1029/2007JA012255.

Kivelson, M., J. Etcheto, and J. Trotignon (1984), Global compressional oscillations of the terrestrial magnetosphere: The evidence and a model, *J. Geophys. Res.*, *89*, 9851, doi:10.1029/JA089iA11p09851.

Kivelson, M. G., M. Cao, R. L. McPherron, and R. J. Walker (1997), A possible signature of magnetic cavity mode oscillations in ISEE spacecraft oscillations, *J. Geomagn. Geoelectr.*, *49*, 1079.

Lessard, M. R., M. K. Hudson, and H. Luhr (1999), A statistical study of Pc3–Pc5 magnetic pulsations observed by the AMPTE/Ion Release Module satellite, *J. Geophys. Res.*, *104*, 4523, doi:10.1029/1998JA900116.

Mann, I. R., et al. (2002), Coordinated ground-based and Cluster observations of large amplitude global magnetospheric oscillations during a fast solar wind speed interval, *Ann. Geophys.*, *20*, 405.

Mathie, R. A., F. W. Menk, I. R. Mann, and D. Orr (1999), Discrete field line resonances and the Alfvén continuum in the outer magnetosphere, *Geophys. Res. Lett.*, *26*, 659, doi:10.1029/1999GL900104.

McPherron, R. L. (2005), Magnetic pulsations: Their sources and relation to solar wind and geomagnetic activity, *Surv. Geophys.*, *26*, 545, doi:10.1007/s10712-005-1758-7.

Morlet, J., G. Arens, E. Fourgeau, and D. Giard (1982), Wave propagation and sampling theory, *Geophysics*, *47*, 203, doi:10.1190/1.1441328.

Orr, D., and J. A. D. Matthew (1971), Variation of geomagnetic micropulsation periods with latitude and plasmapause, *Planet. Space Sci.*, *19*, 897, doi:10.1016/0032-0633(71)90141-3.

Pu, Z. Y., and M. G. Kivelson (1983), Kelvin-Helmholtz instability at the magnetopause: Solution for compressible plasmas, *J. Geophys. Res.*, *88*, 841, doi:10.1029/JA088iA02p00841.

Sarris, T. E., et al. (2009), Characterization of ULF pulsations by THEMIS, *Geophys. Res. Lett.*, *36*, L04104, doi:10.1029/2008GL036732.

Shue, J.-H., J. K. Chao, H. C. Fu, C. T. Russell, P. Song, K. K. Khurana, and H. J. Singer (1997), A new functional form to study the solar wind control of the magnetopause size and shape, *J. Geophys. Res.*, *102*, 9497, doi:10.1029/97JA00196.

Singer, H. J., and M. G. Kivelson (1979), The latitudinal structure of Pc 5 waves in space: Magnetic and electric field observations, *J. Geophys. Res.*, *84*, 7213, doi:10.1029/JA084iA12p07213.

Singer, H. J., D. J. Southwood, R. J. Walker, and M. G. Kivelson (1981), Alfvén wave resonances in a realistic magnetospheric magnetic field geometry, *J. Geophys. Res.*, *86*, 4589, doi:10.1029/JA086iA06p04589.

Takahashi, K., and R. L. McPherron (1982), Harmonic structure of Pc3–4 pulsations, *J. Geophys. Res.*, *87*, 1504, doi:10.1029/JA087iA03p01504.

Takahashi, K., and A. Y. Ukhorskiy (2007), Solar wind control of Pc5 pulsation power at geosynchronous orbit, *J. Geophys. Res.*, *112*, A11205, doi:10.1029/2007JA012483.

Takahashi, K., and A. Y. Ukhorskiy (2008), Timing analysis of the relationship between solar wind parameters and geosynchronous Pc5 amplitude, *J. Geophys. Res.*, *113*, A12204, doi:10.1029/2008JA013327.

Takahashi, K., P. Higbie, and D. N. Baker (1985), Azimuthal propagation and frequency characteristics of compressional Pc5 waves observed at geostationary orbit, *J. Geophys. Res.*, *90*, 1473, doi:10.1029/JA090iA02p01473.

Waters, C. L., B. G. Harrold, F. W. Menk, J. C. Samson, and B. J. Fraser (2000), Field line resonances and waveguide modes at low latitudes: 2. A model, *J. Geophys. Res.*, *105*, 7763, doi:10.1029/1999JA900267.

Yumoto, K., T. Saito, and T. Sakurai (1983), Local time asymmetry in the characteristics of Pc 5 magnetic pulsations, *Planet. Space Sci.*, *31*, 459, doi:10.1016/0032-0633(83)90158-7.

Zhu, X., and M. G. Kivelson (1991), Compressional ULF waves in the outer magnetosphere: 1. Statistical study, *J. Geophys. Res.*, *96*, 19,451, doi:10.1029/91JA01860.

V. Angelopoulos, IGPP, University of California, Los Angeles, CA 90095, USA.

J. Bonnell, Space Sciences Laboratory, University of California, Berkeley, CA 94720, USA.

S. R. Elkington, R. Ergun, X. Li, W. Liu, and T. E. Sarris, Laboratory for Atmospheric and Space Physics, University of Colorado at Boulder, 1234 Innovation Dr., Boulder, CO 80303, USA. (liu@lasp.colorado.edu)

K. H. Glassmeier, IGEP, Technical University of Braunschweig, D-38106 Braunschweig, Germany.